The Plant Cell, Vol. 18, 3171–3181, November 2006, www.plantcell.org

Subcellular Trafficking of the *Arabidopsis* Auxin Influx Carrier AUX1 Uses a Novel Pathway Distinct from PIN1 [W]

Jürgen Kleine-Vehn,[a] Pankaj Dhonukshe,[a] Ranjan Swarup,[b] Malcolm Bennett,[b] and Jiří Friml[a,1]

[a] Center for Molecular Biology of Plants, University of Tübingen, D-72076 Tübingen, Germany
[b] Plant Sciences Division, School of Biosciences, University of Nottingham, Loughborough LE12 5RD, United Kingdom

The directional flow of the plant hormone auxin mediates multiple developmental processes, including patterning and tropisms. Apical and basal plasma membrane localization of AUXIN-RESISTANT1 (AUX1) and PIN-FORMED1 (PIN1) auxin transport components underpins the directionality of intercellular auxin flow in *Arabidopsis thaliana* roots. Here, we examined the mechanism of polar trafficking of AUX1. Real-time live cell analysis along with subcellular markers revealed that AUX1 resides at the apical plasma membrane of protophloem cells and at highly dynamic subpopulations of Golgi apparatus and endosomes in all cell types. Plasma membrane and intracellular pools of AUX1 are interconnected by actin-dependent constitutive trafficking, which is not sensitive to the vesicle trafficking inhibitor brefeldin A. AUX1 subcellular dynamics are not influenced by the auxin influx inhibitor NOA but are blocked by the auxin efflux inhibitors TIBA and PBA. Furthermore, auxin transport inhibitors and interference with the sterol composition of membranes disrupt polar AUX1 distribution at the plasma membrane. Compared with PIN1 trafficking, AUX1 dynamics display different sensitivities to trafficking inhibitors and are independent of the endosomal trafficking regulator ARF GEF GNOM. Hence, AUX1 uses a novel trafficking pathway in plants that is distinct from PIN trafficking, providing an additional mechanism for the fine regulation of auxin transport.

INTRODUCTION

The signaling molecule auxin mediates a surprising variety of plant developmental events, including embryo, root, and vascular tissue patterning, organ and fruit development, tropisms, apical dominance, and tissue regeneration (reviewed in Tanaka et al., 2006). During processes such as tissue regeneration or de novo organ formation, plants rearrange and respecify the polarity of fully specified cells. The connection between cellular polarizing events and the macroscopic manifestation of polarity, such as the specification of different cell types along the axis, largely depends on the directional (polar) transport of auxin (Friml et al., 2003).

Auxin moves actively in a strictly controlled direction from the shoot apex toward the root base by the action of a specialized transport system (reviewed in Benjamins et al., 2005) composed of specific influx and efflux carriers, which mediate auxin flow into and out of cells, respectively. It has been hypothesized that the polarity of auxin flow results from differences at the single cell level between apical and basal membranes in their relative permeabilities to auxin (Rubery and Sheldrake, 1974; Raven, 1975). Candidate genes coding for the critical components of auxin influx and efflux carriers have been identified by molecular genetic studies in *Arabidopsis thaliana*. The components of the auxin efflux complexes of the PIN-FORMED (PIN) family are plasma membrane (PM)–localized, plant-specific proteins that are able to facilitate the efflux of auxin from cells (Petrasek et al., 2006). Importantly, PIN proteins are distributed asymmetrically in auxin transport-competent cells (Gälweiler et al., 1998; Müller et al., 1998; Friml et al., 2002a, 2002b, 2003; Benková et al., 2003), and this polar localization determines the direction of auxin flow at least in meristematic tissues (Wiśniewska et al., 2006).

Physiological experiments indicated that efflux carrier proteins have a very short half-life at the PM (reviewed in Morris, 2000). Molecular–genetic studies confirmed this notion and identified a regulator of subcellular trafficking—GNOM—as a critical component of the delivery of PIN proteins from the endosomes to the PM (Geldner et al., 2001, 2003). *GNOM* (also called *EMB30*) encodes an endosomal, brefeldin A (BFA)–sensitive ARF GEF (for ADP-ribosylation factor GDP/GTP exchange factor) (Shevell et al., 1994), whose inhibition by BFA leads to the disappearance of PINs from the PM and their intracellular accumulation in so-called BFA compartments (Steinmann et al., 1999). This effect is fully reversible and reveals a constitutive cycling of PINs between PM and endosomes (Geldner et al., 2001). Although a biological role for the cycling of PIN proteins is not clarified yet, it may serve as a mechanism for rapid changes in PIN polarity in response to environmental (Friml et al., 2002a) or developmental (Benková et al., 2003; Friml et al., 2003; Reinhardt et al., 2003) cues and as a means of feedback regulation of auxin transport by subcellular PIN translocation (Paciorek et al., 2005).

The auxin influx carrier protein AUXIN-RESISTANT1 (AUX1) belongs to the amino acid permease family of proton-driven transporters and therefore was favored to play a role in the uptake of the Trp-like auxin molecule indole-3-acetic acid (Bennett et al., 1996). The unique features of the phenotype conferred by the *aux1* mutant, which can be rescued specifically

[1] To whom correspondence should be addressed. E-mail jiri.friml@zmbp.uni-tuebingen.de; fax 49-7071-295797.
The author responsible for distribution of materials integral to the findings presented in this article in accordance with the policy described in the Instructions for Authors (www.plantcell.org) is: Jiří Friml (jiri.friml@zmbp.uni-tuebingen.de).
[W] Online version contains Web-only data.
www.plantcell.org/cgi/doi/10.1105/tpc.106.042770

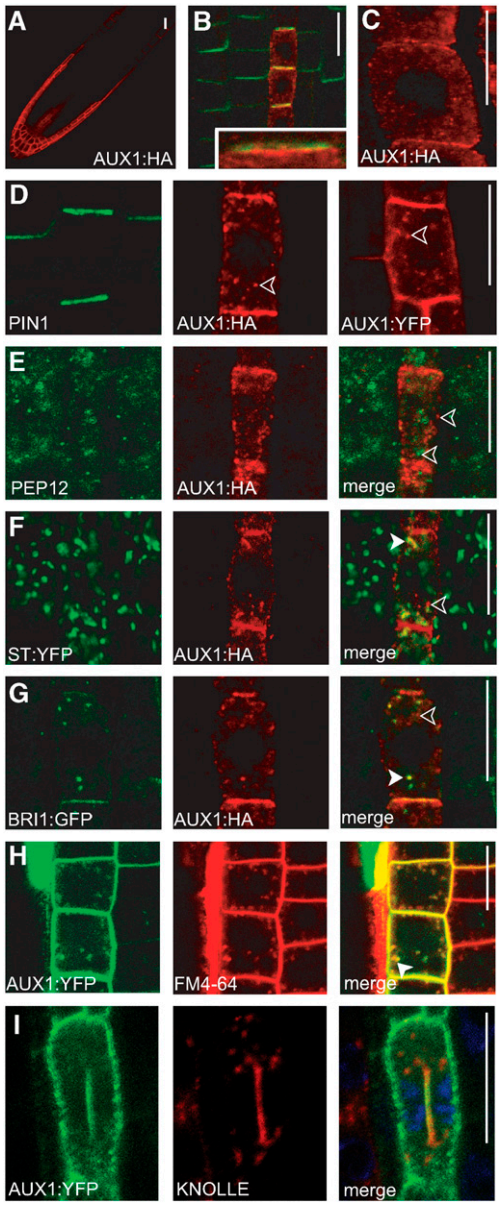

Figure 1. PM and Intracellular Accumulation of AUX1.

(A) to **(C)** Localization of AUX1 (red) and PIN1 (green) auxin transport components.

(A) AUX1 localization pattern in the root tip.

(B) Apical localization of AUX1:HA and basal localization of PIN1 in protophloem cells.

(C) Axial (apical and basal) localization of AUX1:HA in epidermis cells.

(D) AUX1:HA and AUX1:YFP in protophloem cells (red) but not PIN1 (green) show pronounced accumulation in intracellular compartments (indicated by arrowheads).

(E) No colocalization of AUX1:HA (red) and prevacuolar compartment PEP12 (green) in protophloem cells.

(F) Partial colocalization of AUX1:HA (red) and the Golgi apparatus marker ST:YFP (green) in protophloem cells.

(G) Partial colocalization of AUX1:HA (red) and endosomal BRI1:GFP (green) in protophloem cells.

by membrane-permeable auxins, and auxin uptake activity in heterologous systems strongly support the role of AUX1 as an auxin influx carrier (Yamamoto and Yamamoto, 1998; Marchant et al., 1999; Yang et al., 2006). An epitope-tagging approach showed that the AUX1 protein is expressed in protophloem, columella, lateral root cap, and epidermal cells in the *Arabidopsis* root apex (Swarup et al., 2001). Interestingly, in protophloem cells, AUX1 shows a pronounced polar localization at the apical (upper) side of cells (Swarup et al., 2001) opposite to basally (lower side) localized PIN-FORMED1 (PIN1) in the same cells (Friml et al., 2002b). Like PIN proteins, AUX1 localization seems to exhibit BFA sensitivity (Grebe et al., 2002), and AUX1, but not PIN1, trafficking is dependent on the novel endoplasmic reticulum protein, AUXIN-RESISTANT4 (AXR4) (Dharmasiri et al., 2006).

The aim of this study was to characterize AUX1 trafficking and determine its subcellular targeting pathway. Using the unique situation in the protophloem, where AUX1 and PIN1 are polarly localized at the opposite sides of the same cell, the mechanisms of AUX1 and PIN trafficking can be compared. Such data should lead toward a better understanding of the cell biological determinants governing polar auxin transport and also extend our knowledge regarding the apical and basal polar trafficking pathways in plant cells.

RESULTS

AUX1 and PIN1 Localize to the Opposite Sides of Protophloem Cells and Target to the Forming Cell Plate

We analyzed AUX1 subcellular distribution using hemagglutinin (HA)- and yellow fluorescent protein (YFP)–tagged proteins (Swarup et al., 2001, 2004). As shown previously, AUX1 is expressed in epidermis, lateral root cap, columella, and protophloem cells of the root tip (Figure 1A). AUX1 signal can often be found at all cell sides but is regularly enriched at the apical (upper) PM of protophloem cells (Figures 1B and 1D), at both the apical and basal (lower) sides of epidermis cells (Figure 1C), and without pronounced asymmetric distribution in other cell types such as the root cap (see Figure 5J below). By contrast, PIN1 is localized on the basal side of the root stele cells (Friml et al., 2002b), including protophloem (Figure 1B). Importantly, in protophloem cells, AUX1 and PIN1 show localization at opposite sides of the same cell (Figure 1B, inset). PIN proteins (Geldner et al., 2001) along with many other PM proteins (Dhonukshe et al., 2006) have been shown to accumulate in the developing cell plate in dividing cells. Interestingly, AUX1, like PIN1, was detected at cell plates of

(H) Partial colocalization of AUX1:YFP (green) and the endocytic tracer FM4-64 (red) in epidermis cells.

(I) During cell division, AUX1:HA (green) colocalizes at the forming cell plate with KNOLLE (red). 4′,6-Diamidino-2-phenylindole–stained nuclei in protophloem cells are shown in blue.

Immunocytochemistry is shown in **(A)** to **(G)** and **(I)**, and live-cell imaging is shown in **(H)**. Closed arrowheads show colocalizing compartments, and open arrowheads show noncolocalizing compartments (**[E]** to **[H]**). Bars = 10 μm.

dividing protophloem cells, where it colocalized with the cytokinesis-specific syntaxin KNOLLE (Figure 1I).

The occurrence of AUX1 and PIN1 at the opposite sides of protophloem cells suggests that AUX1 and PIN1 are targeted by divergent vesicle trafficking pathways. Furthermore, it indicates that both apical and basal targeting/retrieval operates at the end of cell plate formation, thus establishing PIN1 and AUX1 at opposite sides of the completed cell wall.

AUX1 Also Localizes to the Golgi Apparatus and Endosomes

In addition to their polar PM localization, the protophloem-expressed AUX1:HA and AUX1:YFP fusion proteins exhibit a pronounced intracellular signal (Figure 1D). To characterize the identity of AUX1-labeled endomembranes, we used several established subcellular markers.

No colocalization (Figure 1E; see Supplemental Figure 2 online) was observed with a prevacuolar compartment marker in *Arabidopsis* SYNTAXIN21 (SYP21/PEP12) (da Silva Conceição et al., 1997). By contrast, Golgi apparatus markers γ-COAT PROTEIN (γ-COP) (Ritzenthaler et al., 2002; Geldner et al., 2003) (data not shown) and ST:YFP (Grebe et al., 2003) (Figure 1F; see Supplemental Figure 2 online) exhibited partial colocalization with AUX1:HA signal, suggesting that a percentage of the intracellular AUX1 protein resides at the Golgi apparatus. AUX1 localization at the Golgi apparatus was often variable, suggesting a complex regulation of AUX1 biosynthesis. As PIN proteins are known to recycle between PM and endosomes, we tested whether a proportion of intracellular AUX1 also resides on endosomes. The *Arabidopsis* brassinosteroid receptor BRASSINOSTEROID-INSENSITIVE1 (BRI1) has been reported to reside at the PM and endosomes (Russinova et al., 2004). Simultaneous visualization of BRI1:green fluorescent protein (GFP) and AUX1:HA revealed partial colocalization of intracellular signals (Figure 1G; see Supplemental Figure 2 online).

In other cell types, including epidermal cells, in which AUX1 function has been linked to trichoblast polarity events (Grebe et al., 2002), the intracellular pool of AUX1 was also detected. Real-time, live-cell imaging showed that AUX1:YFP-positive structures are highly dynamic and colocalize with the endocytic tracer lipophilic dye FM4-64 at early stages (<5 min) of its internalization (Figure 1H; see Supplemental Movie 1 online). This further confirms that part of intracellular AUX1 resides in endosomes. Collectively, these data show that the intracellular pool of AUX1 resides on both dynamic endosomal and Golgi apparatus membranes.

Intracellular but Not PM AUX1 Localization Is BFA Sensitive

In *Arabidopsis*, BFA blocks trafficking from recycling endosomes to the PM and causes endosomes and internalized endocytic cargo to aggregate into so-called BFA compartments, which become surrounded by Golgi stacks (Geldner et al., 2003). It has been shown previously that both PIN1 and AUX1 accumulate in BFA compartments (Geldner et al., 2001; Grebe et al., 2002).

PIN1 and AUX1 aggregation in BFA compartments is fully reversible, as removal of BFA in the presence of the protein synthesis inhibitor cycloheximide (50 μM, 1 h) leads to the reestablishment of PIN1 (Geldner et al., 2001) and AUX1 localization at the PM and subcellular structures (see Figure 4A below). In addition, latrunculin B (Lat B)–dependent depolymerization of the actin cytoskeleton inhibits PIN1 and AUX1 accumulation in BFA compartments (Geldner et al., 2001) (data not shown), confirming the BFA-sensitive, actin-dependent distribution of PIN1 and AUX1 proteins.

Next, we compared the dynamics of PIN1 and AUX1 translocation in response to BFA. PIN1 was almost completely internalized within 2 h (i.e., the signal disappeared from the basal PM and appeared in BFA compartments) (Figure 2A). Under similar conditions (50 μM BFA, 2 h), AUX1 showed weak intracellular agglomeration, with the majority of the AUX1 signal remaining at the PM (Figure 2A). Even at higher BFA concentrations (up to 200 μM) and extended treatment periods (up to 6 h), the AUX1 signal strongly persisted in the PM (data not shown). Moreover, PM localization of AUX1 in epidermis cells also persisted after prolonged BFA treatment (see Figures 4A and 4B below), suggesting a similar, BFA-resistant targeting mechanism to the PM in both cell types.

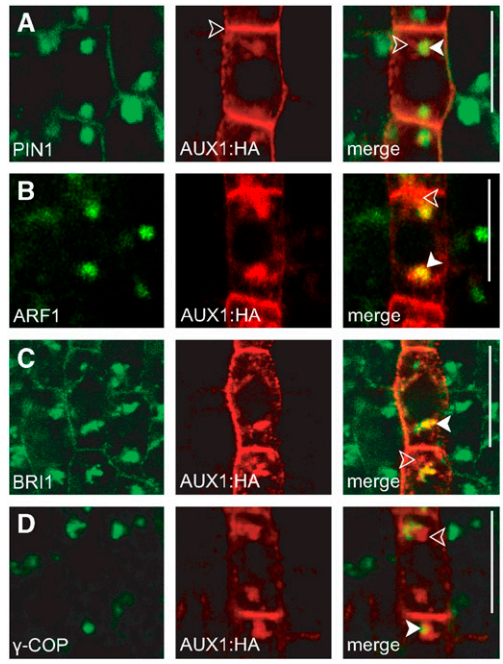

Figure 2. BFA-Sensitive Dynamics of AUX1 in Protophloem Cells.

(A) Partial colocalization of PIN1 (green) and AUX1:HA (red) in BFA compartments.

(B) Partial colocalization of endosomal ARF1 (green) and AUX1:HA (red) in BFA compartments.

(C) Partial colocalization of endosomal BRI1:GFP (green) and AUX1:HA (red) in BFA compartments.

(D) Partial colocalization of the Golgi marker γ-COP (green) and AUX1:HA (red) in BFA compartments.

Closed arrowheads show colocalizing compartments, and open arrowheads show noncolocalizing compartments. Immunocytochemistry imaging is shown in all panels. Bars = 10 μm.

Furthermore, although the typical PIN1 signal in BFA compartments was uniformly rounded, the AUX1 accumulation in protophloem cells was more dispersed and irregularly shaped. Colocalizations after BFA treatment (50 μM BFA, 2 h) showed that PIN1 partially colocalized with AUX1, often in the center of the BFA compartments (Figure 2A; see Supplemental Figure 2 online). Here also, the endosomal markers BRI1 and ADP-RIBOSYLATION FACTOR1 (ARF1) (Xu and Scheres, 2005) showed pronounced colocalization with internalized PIN1 (Paciorek et al., 2005), whereas only partial colocalization was observed with AUX1 in BFA compartments (Figures 2B and 2C; see Supplemental Figures 2 and 3 online). On the other hand, the Golgi apparatus markers γ-COP and ST:YFP did not colocalize with PIN1 in BFA compartments (Geldner et al., 2003) but showed partial colocalization with AUX1 (Figure 2D; data not shown; see Supplemental Figure 2 online). In accordance with the PEP12/AUX1 colocalization study, PEP12 did not colocalize with BRI1 in BFA compartments (see Supplemental Figure 1 online).

These findings confirm that AUX1 accumulates in BFA compartments. However, this relates to the aggregation of AUX1-containing endosomal and Golgi apparatus–derived structures. In contrast with PIN1, the prolonged BFA treatments did not visibly affect AUX1 localization at the PM, suggesting a BFA-resistant mechanism of AUX1 targeting to the PM.

Fluorescence Recovery after Photobleaching Analysis Reveals a Connection between Intracellular and PM Pools of AUX1

Unlike in the case of PIN1 (Geldner et al., 2001), the BFA treatment experiments did not unambiguously demonstrate a constitutive endosomal recycling of AUX1 to and from the PM.

To examine whether there is any exchange of AUX1 between the PM and the intracellular pool, we performed fluorescence recovery after photobleaching (FRAP) experiments. In protophloem and epidermis cells, the PM pool of AUX1:YFP recovered visibly within 20 min after bleaching (Figures 3A and 3D). Because TIBA (50 μM, 1 h), which inhibits actin-dependent protein recycling (Geldner et al., 2001), impeded AUX1 recovery at the PM (Figure 3F; see Supplemental Figure 4 online), we concluded that AUX1 recovery is conditioned by trafficking-dependent delivery rather than by lateral diffusion. This is in accordance with the constant arrival of AUX1-containing intracellular structures at the PM, as visualized by live-cell imaging (see Supplemental Movie 1 online). When protein synthesis was inhibited by cycloheximide (50 μM, 0.5 h) (Geldner et al., 2001), the recovery of AUX1 at the PM was slower but nevertheless occurred within 30 min (Figure 3B). This finding shows that the PM pool can be replenished by AUX1 from the preexisting intracellular pool.

When the PM pool of AUX1:YFP in protophloem cells was bleached and the cells were cotreated with BFA, AUX1 still accumulated in BFA compartments (Figure 3C), confirming only an insignificant contribution of PM-localized AUX1 to BFA compartments. Importantly, in this case (Figure 3C) and also when cells were pretreated with BFA (50 μM, 1 h) (Figure 3E), we still observed AUX1 recovery at the PM after 20 to 30 min in both protophloem and epidermis cells.

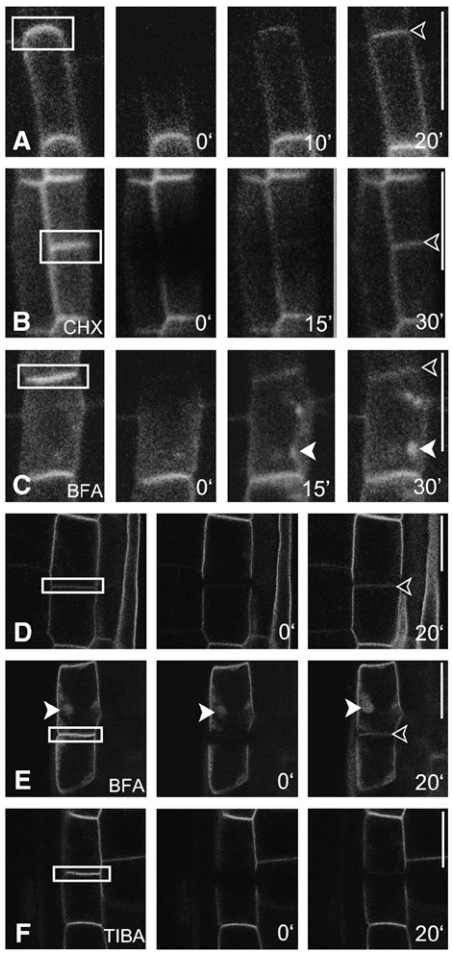

Figure 3. FRAP Analysis of AUX1 Dynamics.

FRAP analysis of AUX1:YFP in protophloem (**[A]** to **[C]**) and epidermal cells (**[D]** to **[F]**).

(A) AUX1:YFP incidence at the apical PM of protophloem cells recovers within 20 min after photobleaching.

(B) AUX1:YFP recovery at the apical PM is delayed (30 min) when protein synthesis is inhibited by cycloheximide (CHX).

(C) AUX1:YFP label also accumulates in BFA compartments when the PM pool of AUX1 is photobleached. The recovery at the PM also occurs to some extent in the presence of BFA.

(D) AUX1:YFP recovery in untreated epidermal root cells after 20 min.

(E) AUX1:YFP recovery at the PM after BFA compartment formation occurs within 20 min.

(F) TIBA interferes with AUX1:YFP recovery at the PM.

Open arrowheads depict recovered AUX1 at the PM, and closed arrowheads depict recovered AUX1 at the BFA compartments. Bars = 10 μm.

Hence, the intracellular and PM pools of AUX1 are interconnected, but AUX1 protein delivery to the PM is BFA-insensitive and AUX1 occurrence in the BFA compartments is to a large extent attributable to the fusion of the intracellular Golgi apparatus and endosomal membranes containing AUX1 protein. Thus, in contrast with PIN1, which needs the action of BFA-sensitive ARF GEF GNOM, constitutive AUX1 delivery to the PM likely involves BFA-resistant ARF GEFs.

Subcellular Trafficking of AUX1 Is GNOM Independent

Although the delivery of AUX1 to the PM seems to involve BFA-resistant ARF GEFs, AUX1 subcellular dynamics also require the activity of BFA-sensitive ARF GEFs (Grebe et al., 2002), as the intracellular AUX1 pool reversibly accumulates in BFA compartments (Figure 4A). We addressed whether this process involves the BFA-sensitive ARF GEF GNOM, which is a major ARF GEF involved in the trafficking of PIN proteins (Geldner et al., 2003). AUX1:YFP was coexpressed in a transgenic line in which the wild-type GNOM protein was replaced by the BFA-resistant GNOM (GN) version (GN^{M696L}-myc) (Geldner et al., 2003). The delivery of PIN1 to the PM is to a large extent BFA-resistant in this line, as BFA treatment does not lead to the accumulation of PIN1 in the BFA compartments (Geldner et al., 2003). By contrast, AUX1:YFP still readily accumulated in BFA compartments after BFA (50 μM, 2 h) treatment in GN^{M696L}-myc transgenic lines in both epidermis and protophloem cells (Figure 4B, inset). Moreover, the protein amount and time dependence was fully comparable to AUX1 accumulation in the wild-type control. This demonstrates that the BFA-induced agglomeration of AUX1, unlike PIN1, is independent of GNOM function and requires the action of other BFA-sensitive ARF GEFs. This observation further emphasizes the differences in the mechanisms of PIN1 and AUX1 trafficking.

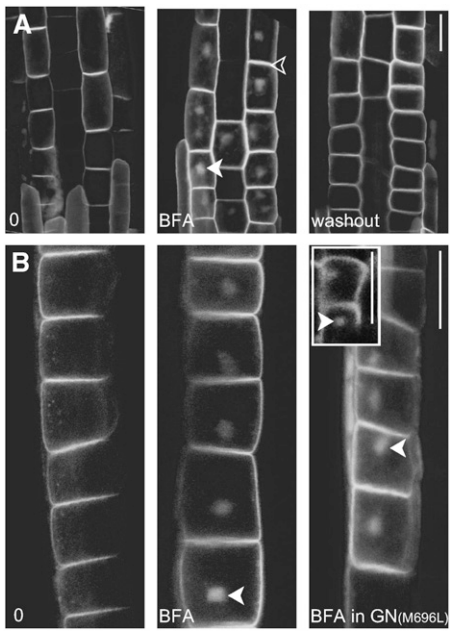

Figure 4. GNOM-Independent Dynamics of AUX1 in Epidermal Cells.

(A) AUX1:YFP shows reversible accumulation in BFA compartments after BFA treatment.

(B) AUX1:YFP also readily accumulates in BFA compartments in the BFA-resistant GNOM line. The inset shows the BFA-dependent accumulation of AUX1:YFP in protophloem cells.

The open arrowhead indicates that AUX1 remains constant at the PM, and closed arrowheads indicate BFA compartments. Live-cell imaging is shown in all panels. Bars = 10 μm.

AUX1 Localization and Intracellular Dynamics Require the Actin Cytoskeleton

Next, we analyzed the cytoskeletal requirements for the guidance of AUX1-containing vesicles. We interfered with the cytoskeleton using the microtubule-depolymerizing agent oryzalin (Hugdahl and Morejohn, 1993) and the actin depolymerizer Lat B (Spector et al., 1983). A similar experimental strategy previously revealed that PIN protein dynamics primarily require actin filaments but not microtubules (Geldner et al., 2001; Friml et al., 2002a).

Oryzalin treatments (20 μM, 3 h) were sufficient to disrupt microtubules (Geldner et al., 2001) but did not visibly interfere with AUX1 trafficking. Only treatments with high oryzalin concentrations (40 μM, 3 h), which lead to changes in cell morphology and therefore might induce secondary effects, affected AUX1 polar localization (see Supplemental Figure 5 online). These results suggest that microtubules are not primarily required for AUX1 polar localization and subcellular dynamics.

By contrast, actin depolymerization by Lat B (30 μM, 3 h) led to intracellular agglomeration of the AUX1 signal in protophloem (Figure 5B) or epidermis (data not shown) cells. Lat B treatments also affected the polarity of PIN1 and AUX1 localization to some extent, as treated seedlings showed more randomly distributed PIN1 and AUX1 signals in protophloem cells (Figure 5B). Furthermore, analysis of the concentration dependence of the Lat B effect showed that a lower Lat B concentration (20 μM, 3 h), which did not affect PIN1 localization, was sufficient to strongly influence AUX1 targeting (Figure 5A).

In summary, these data show that AUX1 trafficking and polar PM localization are not strictly dependent on microtubules but require intact actin filaments. Moreover, AUX1 localization at the PM is more strictly dependent on the actin cytoskeleton than is PIN1 localization.

Effects of Auxin Transport Inhibitors on AUX1 Dynamics

Auxin has been shown to inhibit the endocytic step of PIN cycling (Paciorek et al., 2005). In addition, auxin efflux inhibitors such as TIBA and PBA interfere with the intracellular cycling of PIN proteins (Geldner et al., 2001). Recently, another class of inhibitors, such as 1-NOA, which preferentially targets auxin influx, has been identified, but the molecular mechanism of their action remains unknown (Parry et al., 2001). However, all of these inhibitors interfere with auxin transport–dependent auxin distribution within tissues, as monitored by DR5-based auxin response reporters (Sabatini et al., 1999; Ottenschläger et al., 2003).

We tested the effects of auxin efflux and influx inhibitors on AUX1 trafficking. It appeared that efflux-dependent auxin flow is necessary for the polar PM localization of AUX1 and PIN1, because treatments with the auxin efflux inhibitor naphthylphthalamic acid (50 μM, 3 h) largely abolished the polar localization of both proteins (Figure 5D). On the other hand, inhibition of influx by 1-NOA treatment, even at high concentrations (100 μM, 3 h), did not interfere substantially with polar PM or intracellular localization of AUX1 or PIN1 (Figure 5E). Moreover, both PIN1 and AUX1 readily accumulated in BFA compartments in the

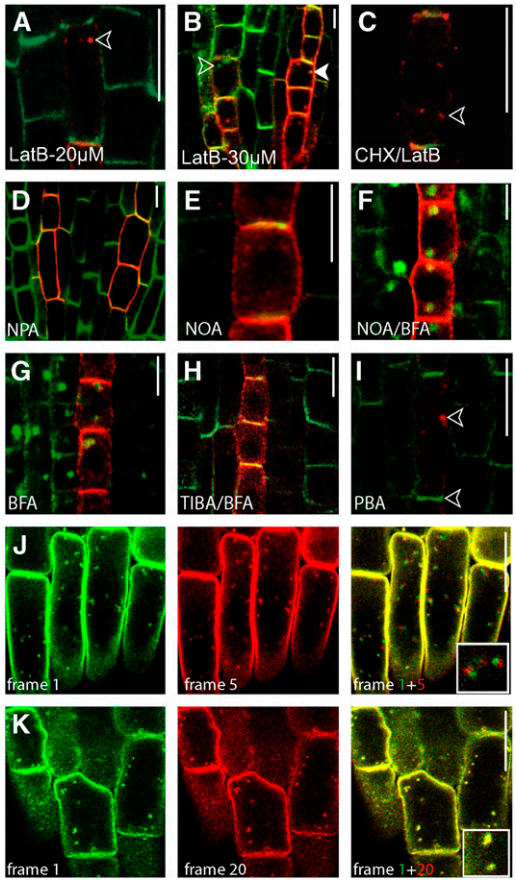

Figure 5. Auxin and Auxin Transport Inhibitors: Effects on AUX1 Dynamics.

(A) The actin-depolymerizing agent Lat B preferentially targets AUX1 and causes AUX1 retrieval from the PM and its aggregation.
(B) At higher Lat B concentrations, PIN1 is also affected.
(C) AUX1 aggregation also occurs when protein synthesis is inhibited. CHX, cycloheximide.
(D) Naphthylphthalamic acid (NPA) affects the polar distribution of AUX1 and PIN1.
(E) 1-NOA does not affect the localization of AUX1 and PIN1.
(F) AUX1 and PIN1 readily accumulate in BFA compartments in the presence of 1-NOA.
(G) BFA treatment leads to AUX1/PIN1 accumulation in BFA compartments.
(H) TIBA inhibits the BFA-induced aggregation of AUX1/PIN1.
(I) PBA treatment causes the internalization and subcellular aggregation of AUX1 but not of PIN1 (indicated by the lower arrowhead).
(J) Subcellular dynamics of AUX1:YFP (yellow). Overlay of frame 1 (green) on frame 5 (+30 s; red).
(K) TIBA blocks the subcellular dynamics of AUX1:YFP. Overlay of frame 1 (green) on frame 20 (+120 s; red).
Open arrowheads indicate AUX1 accumulation, and the closed arrowhead shows AUX1/PIN1 colocalization. Immunocytochemistry of protophloem cells is shown in **(A)** to **(I)**, and live-cell imaging of lateral root cap cells is shown in **(J)** and **(K)**. The localization of AUX1:HA is shown in red, and that of PIN1 is shown in green in **(A)** to **(I)**. Bars = 10 μm.

presence of 1-NOA in protophloem (Figure 5F) and epidermal (see Supplemental Figure 6A online) cells. These results suggest that the 1-NOA inhibition of auxin influx is not attributable to an effect on AUX1 polarity or trafficking.

By contrast, TIBA and PBA have profound effects on AUX1 trafficking. TIBA (50 μM, 30-min pretreatment) inhibited the BFA-induced (50 μM, 2 h) aggregation of AUX1 in protophloem (Figures 5G and 5H) and epidermis (see Supplemental Figure 6B online). Furthermore, the recovery of AUX1 from the BFA compartments was completely inhibited when BFA was washed out with TIBA or PBA (see Supplemental Figure 6C online). These results suggest that both TIBA and PBA inhibit trafficking not only of PIN1 (Geldner et al., 2001) but also of AUX1. To test directly the effect of these drugs on AUX1 trafficking, we performed live-cell imaging experiments in the absence and presence of these drugs. In the lateral root cap cells, AUX1:YFP-labeled membranes displayed highly dynamic behavior (see Supplemental Movie 1 online), which was visualized by a superimposition of successive frames 1 and 5 (6-s interval between frames, color-coded green and red; Figure 5J). Strikingly, in the presence of TIBA (50 μM) or PBA (10 μM), AUX1 motility was blocked (see Supplemental Movie 2 online and the superimposition of frames 1 and 20 in Figure 5K). By contrast, treatment with auxins (50 μM naphthylacetic acid) did not influence AUX1 dynamics (see Supplemental Movie 3 and Supplemental Figures 6E to 6G online). Inhibition of AUX1 dynamics for a prolonged period (PBA, 5 μM, 3 h; TIBA, 50 μM, 5 h) led to subcellular aggregation of AUX1 in the protophloem (Figure 5I) and epidermis (data not shown). These effects seem to be more specific for AUX1 trafficking, because PIN1 localization is affected to a much lesser extent and only at higher concentrations or longer treatments.

These data collectively demonstrate that TIBA and PBA, but not 1-NOA or auxins, block the subcellular trafficking of the AUX1 protein. Moreover, AUX1 trafficking is more sensitive than PIN1 to PBA/TIBA action, which may reflect stricter requirements for AUX1 trafficking along actin filaments and/or actin-dependent protein anchoring of AUX1 at the PM.

Sterol Composition of Membranes Affects AUX1 Targeting

Sterols are known to be important for polar sorting events in animal cells (Keller and Simons, 1998; Michaux et al., 2000). Recent studies suggested sterol involvement in polar protein targeting in plant cells, as PIN1 polarity was perturbed in the *orc* mutant, which is deficient in STEROL METHYLTRANSFERASE1 (SMT1) function (Willemsen et al., 2003). In animals, filipin specifically binds sterols (Miller, 1984), and high filipin doses are known to shift or deplete sterols in membranes of animal cells, leading to the inhibition of endocytosis (Marella et al., 2002). In plant cells, filipin also binds sterols (Grebe et al., 2003) and inhibits FM4-64 uptake as well as the endocytosis of PM-resident proteins (Figures 6A to 6E), suggesting a comparable mode of filipin action in animal and plant cells.

Filipin treatment (100 μM, 1.5 h) leads to strong AUX1 accumulation in aggregates preferentially associated with the lateral PM in protophloem (Figure 6F) but not in epidermis or lateral root cap cells (see Supplemental Figure 7 online). In the case of PIN1, filipin interfered slightly with polar localization, but no lateral

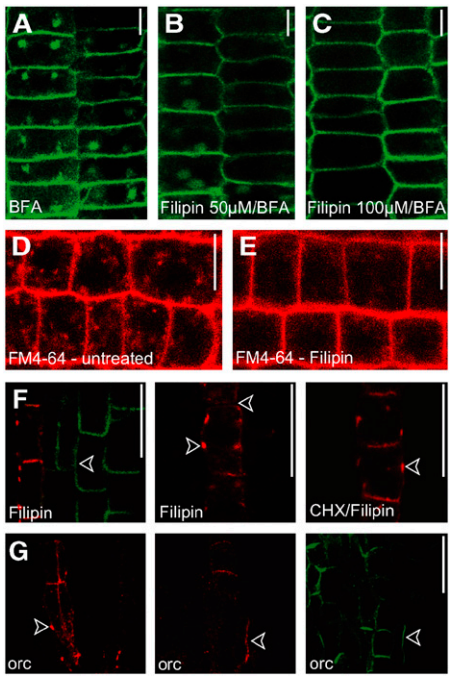

Figure 6. Sterol Requirements of AUX1 and PIN1 Dynamics.

(A) Aquaporin PIP2:GFP-expressing epidermal root cells show accumulation in BFA compartments.
(B) Pretreatment with 50 μM filipin shows weak effects on BFA-induced internalization of PIP2.
(C) Filipin treatment (100 μM) prevents PIP2 accumulation in BFA compartments.
(D) FM4-64 uptake (35 min) in untreated epidermal root cells.
(E) FM4-64 uptake (35 min) in filipin-treated (100 μM) epidermal root cells.
(F) The sterol binding agent filipin preferentially targets AUX1 and leads to AUX1 aggregation predominantly at the lateral cell sides. The polarity of PIN1 localization also is affected. AUX1 aggregation also occurs when protein synthesis is inhibited. CHX, cycloheximide.
(G) Genetic interference with sterol composition in *orc* mutants leads to AUX1 and PIN1 polarity defects and AUX1 aggregation.
Immunocytochemistry imaging is shown in **(A)** to **(C)**, **(F)**, and **(G)**, and live-cell imaging of epidermis cells is shown in **(D)** and **(E)**. The localization of AUX1:HA is shown in red, and that of PIN1 is shown in green in **(F)** and **(G)**. Arrowheads indicate ectopic localization. Bars = 10 μm.

agglomeration was observed (Figure 6F). Similarly, genetic interference with sterol composition in the *orc* mutant leads to changes in PIN polarity (Willemsen et al., 2003) and AUX1 localization, also resulting in lateral AUX1 agglomeration (Figure 6G).

Thus, pharmacological and genetic interference with sterols leads to defects in PIN1 and AUX1 polarity and agglomeration of AUX1, suggesting that AUX1 trafficking in protophloem cells strictly requires sterol function. The alternative possibility, that sterol depletion–based mislocalization of PIN proteins leads to alterations in auxin distribution and this, in turn, affects AUX1 trafficking, is unlikely because pharmacological inhibition of auxin transport does not have comparable effects on AUX1 localization (Figure 5E).

DISCUSSION

Mapping the AUX1 Trafficking and Polar Targeting Pathways

The combination of pharmacological, genetic, and live-cell imaging approaches in our studies have revealed a pathway for subcellular trafficking and polar targeting of the AUX1 auxin influx carrier. In protophloem cells, localization of AUX1 is polarized to some extent, with increased amounts of protein found at the upper (apical) PM (Swarup et al., 2001). In addition to this cell surface pool, a smaller proportion of AUX1 is also located intracellularly in the Golgi apparatus and endosomes. The Golgi apparatus–localized AUX1 most likely represents newly synthesized protein, consistent with the finding that the intracellular pool, as well as the recovery of AUX1 at the PM, decreases after the inhibition of protein synthesis. By contrast, the endosomal pool of AUX1 is possibly related to the constitutive recycling of AUX1 to and from the PM. The FRAP analysis of live cells showed an intensive exchange of AUX1 between the PM and the intracellular pool and that this exchange is independent of the synthesis of new protein. It has emerged from multiple studies that in plants, the vesicular motility in interphase cells is based mainly on the actin cytoskeleton (Geldner et al., 2001; Voigt et al., 2005). In accordance, the intracellular AUX1 dynamics strictly require an intact actin cytoskeleton but are only marginally, if at all, dependent on microtubules. Furthermore, the maintenance of the apical PM localization of AUX1 is dependent on the actin cytoskeleton and the sterol composition of the membranes. Unlike PIN1, this constitutive trafficking cannot be visualized using the vesicle trafficking inhibitor BFA, as the delivery of AUX1 to the PM can occur independently of BFA-sensitive ARF GEFs, including ARF GEF GNOM. On the other hand, the subcellular dynamics of the intracellular AUX1 pool requires an as yet unknown BFA-sensitive ARF GEF, as demonstrated by the aggregation of the intracellular endosomal and Golgi apparatus AUX1 pools into BFA compartments. This suggests a complex action of BFA-sensitive and -resistant ARF GEFs at different steps of subcellular AUX1 trafficking and explains the apparent discrepancy that AUX1 trafficking is BFA-sensitive (Grebe et al., 2002) yet auxin influx is BFA-insensitive, in contrast with auxin efflux (Morris and Robinson, 1998).

AUX1 and PIN Trafficking Pathways Are Distinct

Our studies have revealed a constitutive movement of the AUX1 auxin influx component between the PM and the intracellular endosomal pool. Such dynamics share important features with PIN proteins, the constitutive cycling components of auxin efflux. PIN1 trafficking, which, like AUX1 trafficking, can be polar or nonpolar, depending on the cell type (Friml et al., 2002a, 2002b), occurs along the actin cytoskeleton rather than along microtubules (Geldner et al., 2001) and is dependent on the sterol composition of the membranes (Willemsen et al., 2003). The trafficking of the PIN1 vesicles to the PM requires the action of the BFA-sensitive endosomal ARF GEF GNOM (Geldner et al., 2003). Normally, the equilibrium of the cell surface and intracellular pools of PIN1 protein is shifted in favor of the PM pool, so the

intracellular PIN1 is difficult to visualize (Paciorek et al., 2005). By contrast, AUX1 can be more easily detected in intracellular endomembranes consisting partly of Golgi apparatus and endosomes. This population of AUX1 is targeted in a GNOM-independent manner and also in a BFA-resistant manner, at least in trafficking to the PM (Figure 7).

Notably, AUX1 targeting is more sensitive than PIN targeting to interference with the actin cytoskeleton and its dynamics. In addition, a sterol membrane composition is important for AUX1 delivery, as genetic or chemical interference with sterols leads to the retrieval of AUX1 from the PM and its aggregation. Such a sterol–AUX1 relationship is reminiscent of the sterol dependence of apical targeting in epithelial cells. There, selected proteins associate with lipid rafts during apical targeting, with rafts consequently acting as apical sorting platforms (Schuck and Simons, 2004). In animal cells, filipin has been used to specifically interfere with the formation of caveolae and the subsequent inhibition of clathrin-independent endocytosis (Nabi and Le, 2003). Further investigation will clarify whether filipin effects on AUX1 targeting underlie the same caveolae-like endocytosis mechanism in plant cells. In conclusion, the different cell biological requirements of delivery to the PM show that PIN proteins and AUX1 use distinct trafficking pathways. Furthermore, the secretory pathway of the newly synthesized AUX1 from the endoplasmic reticulum is distinct from the PIN1 secretory pathway, as demonstrated by analysis of the role of the endoplasmic reticulum–resident AXR4 protein (Dharmasiri et al., 2006). Thus, AUX1 trafficking represents a novel pathway for the delivery and constitutive trafficking of PM proteins in plants. It seems that AUX1 trafficking also uses similar mechanisms in cell types in which AUX1 is not polarly localized. This suggests that the observed differences in the targeting mechanism reflect specific differences between AUX1 and PIN1 targeting rather than a general difference between apical and basal targeting pathways in plants.

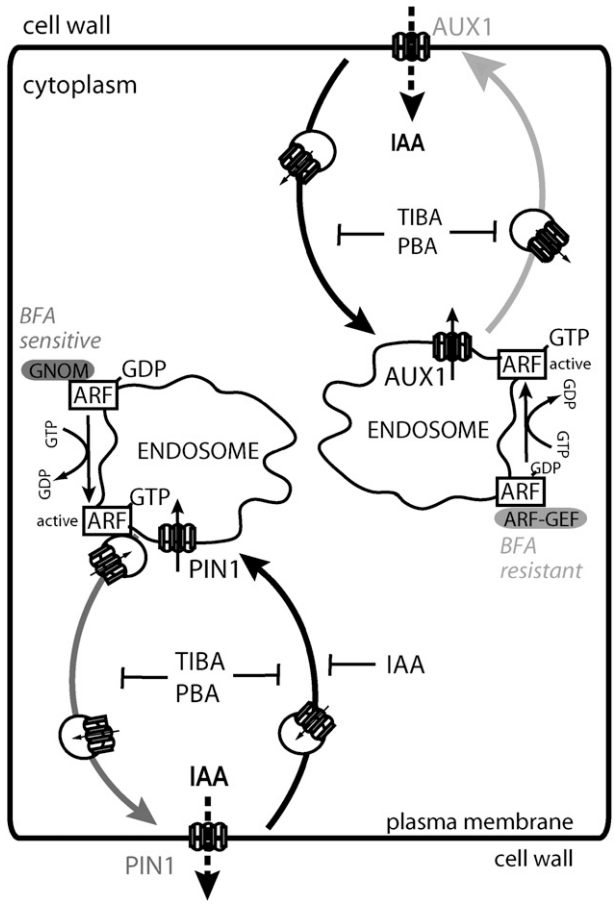

Figure 7. Model of Distinct Pathways for the Constitutive Trafficking of AUX1 and PIN1.

PIN1 and AUX1 are targeted in protophloem cells to distinct polar domains. Both proteins display actin-dependent, TIBA/PBA-sensitive constitutive trafficking between endosomes and the PM, although AUX1 trafficking is more sensitive to TIBA/PBA and actin depolymerization. PIN1 delivery to the PM requires BFA-sensitive, endosomal ARF GEF GNOM, whereas AUX1 trafficking depends on another BFA-resistant ARF GEF. In addition, there is another endosomal, BFA-sensitive ARF GEF (not indicated here) whose inhibition by BFA leads to the aggregation of AUX1-bearing endosomes. The arrows associated with AUX1 and PIN1 proteins show the orientation of these proteins with regard to the direction of transport. It is unclear, however, whether AUX1 and PIN1 also can be active when internalized. IAA, indole-3-acetic acid.

Functional Relevance of AUX1 and PIN Trafficking

We conclude from our studies that AUX1 and PIN1 proteins are trafficked by distinct pathways (Figure 7). Independent targeting of AUX1 and PIN1 provides several functional advantages. First, AUX1 and PIN1 proteins can adopt distinct patterns of localization in the same cell or different cell types to fine-tune polar auxin transport for a particular developmental purpose. For example, AUX1 and PIN1 are targeted to opposite ends of protophloem cells to facilitate the intercellular transport of auxin from the phloem to the root apical meristem. By contrast, colocalization of AUX1 and PIN1 at the same side of L1 cells on the flanks of the shoot apical meristem is hypothesized to create an auxin maximum at this position, demarcating the position of a new leaf primordium (Reinhardt et al., 2003). Second, targeting AUX1 and PIN1 by distinct pathways provides the opportunity to regulate their trafficking independently. For example, PIN recycling is regulated by auxin (Paciorek et al., 2005), whereas AUX1 trafficking seems to be unrelated to auxin. This distinction allows positive feedback by increased intracellular auxin levels on auxin efflux but not influx. This homeostatic mechanism appears entirely logical, as it does not interfere with the AUX1-dependent redistribution of auxin between tissues, which was recently demonstrated to be critical for root gravitropism (Swarup et al., 2005). Hence, the independent regulation of the trafficking of auxin influx and efflux components enables the fine-tuning of polar auxin transport in response to multiple cues and provides an additional level of regulation of this crucial physiological process.

In conclusion, our results provide evidence for the existence of different pathways for the polar targeting of apical and basal cargos in plant cells. Additionally, they also provide AUX1 and PIN1 as model substrates for the further molecular analysis of these distinct trafficking pathways.

METHODS

Plant Material and Growth Conditions

Arabidopsis thaliana plants and seedlings (ecotype Columbia) were grown in growth chambers under long-day conditions at 23°C. Experiments were performed on 5-d-old seedlings grown on vertically oriented plates containing *Arabidopsis* medium (half-strength Murashige and Skoog agar and 1% sucrose, pH 5.8). Incubation of seedlings with various chemicals was performed on 24-well cell culture plates containing the indicated concentrations of chemicals in *Arabidopsis* medium. If not indicated differently, the following conditions were used. Conditional pretreatment for 0.5 h with the first drug was followed by 2 to 3 h of concomitant second drug treatment. Control treatments contained equal amounts of solvent (DMSO or ethanol). The following mutants and transformants have been described previously: *ST:YFP* (Grebe et al., 2003); BRI1:GFP (Russinova et al., 2004); AUX1:HA (Swarup et al., 2001); AUX1:YFP (Swarup et al., 2004); *GNOM*^{M696L}*-myc* (Geldner et al., 2003); and *orc* (Willemsen et al., 2003).

Expression and Localization Analysis

Whole-mount immunofluorescence preparations were assembled as described (Friml et al., 2003). The rabbit anti-PIN1 polyclonal antiserum was raised against amino acids 288 to 452 of PIN1 and used previously for PIN1 localization in tissue sections (Benková et al., 2003; Reinhardt et al., 2003). For whole-mount immunolocalization in roots, immunoglobulins from the crude serum were precipitated by saturated $(NH_4)_2SO_4$ solution (2:1) and dialyzed against PBS. The purified fraction was diluted 1:1000. Other antibodies were diluted as follows: anti-GFP (1:300; Molecular Probes), anti-HA (1:600; SantaCruz), anti-PEP12 (1:200; da Silva Conceicao et al., 1997), anti-ARF1 (1:1000; Pimpl et al., 2000); anti-At γ-COP (1:1000; Movafeghi et al., 1999), and anti-KNOLLE (1:500; Lauber et al., 1997). Fluorescein isothiocyanate– and Cy3-conjugated anti-rabbit secondary antibodies (Dianova) were diluted 1:500, and 1:600, respectively, and YFP was visualized in 5% glycerol without fixation (live-cell imaging). For confocal laser scanning microscopy, a Leica TCS SP2 microscope was used. Images were processed in Adobe Photoshop cs. Profile analyses of the BFA compartment were performed with Leica Confocal Software. For quantification of colocalization, intracellular signals in protophloem cells were marked ($n = 6$), and total pixels of both channels and merged pixels were counted (phyton-based). Subsequently, the percentage of overlaying signal for both proteins was determined, and statistical analysis was performed using Microsoft Office Excel 2003.

Live-Cell Imaging and FRAP Analysis

Live-cell imaging and FRAP analysis were performed using a confocal microscope (model TCS SP2; Leica) equipped with an He-Cd laser and an argon laser (which provides excitation at 514 nm for YFP). For the photobleaching experiment, a region of interest was selected for scans using the Leica FRAP procedure. YFP images before and after scans were collected. All FRAP analyses were performed with Leica Confocal Software.

Accession Numbers

Arabidopsis Genome Initiative locus identifiers for the genes mentioned in this article are as follows: ARF1 (At1g23490), AUX1 (At2g38120), BRI1 (At4g39400), γ-COP/SEC21p (At4g34450), GNOM (At1g13980), KNOLLE (At1g08560), PEP12 (At5g16830), PIN1 (At1g73590), and SMT1 (At5g13710).

Supplemental Data

The following materials are available in the online version of this article.

Supplemental Movie 1. Dynamics of AUX1-YFP in *Arabidopsis* Lateral Root Cap Cells.

Supplemental Movie 2. TIBA Inhibits the Dynamics of AUX1-YFP in *Arabidopsis* Lateral Root Cap Cells.

Supplemental Movie 3. Auxin Does Not Visibly Interfere with the Dynamics of AUX1-YFP in *Arabidopsis* Lateral Root Cap Cells.

Supplemental Figure 1. The PVC Marker PEP12 Does Not Colocalize with the Endosomal Marker in *Arabidopsis*.

Supplemental Figure 2. Evaluation of the Colocalization of AUX1:HA and a Subcellular Marker.

Supplemental Figure 3. Intensity Profile Analysis of AUX1 and Subcellular Markers in BFA Compartments.

Supplemental Figure 4. FRAP Charts of AUX1 Dynamics.

Supplemental Figure 5. Oryzalin Does Not Interfere with AUX1/PIN1 Targeting.

Supplemental Figure 6. Effects of Auxin Transport Inhibitors on AUX1 in Epidermis Cells.

Supplemental Figure 7. Filipin Effects on AUX1 in Epidermis and Lateral Root Cap Cells.

ACKNOWLEDGMENTS

We are very grateful to Gregor Nobis for technical assistance, David Robinson for sharing antibody-based subcellular markers, and Annika Sunnanväder for critical reading of the manuscript. This work was supported by the Volkswagenstiftung (J.F., J.K.-V., and P.D.), the European Molecular Biology Organization Young Investigator Program (J.F.), institutional support (MSM0021622415 to J.F.), the Friedrich Ebert Stiftung (J. K.-V.), and by Biotechnology and Biological Science Research Council and Gatsby Charitable Foundation funding to M.B. and R.S.

Received March 28, 2006; revised September 11, 2006; accepted October 26, 2006; published November 17, 2006.

REFERENCES

Benjamins, R., Malenica, N., and Luschnig, C. (2005). Regulating the regulator: The control of auxin transport. Bioessays **27,** 1246–1255.

Benková, E., Michniewicz, M., Sauer, M., Teichmann, T., Seifertova, D., Jurgens, G., and Friml, J. (2003). Local, efflux-dependent auxin gradients as a common module for plant organ formation. Cell **115,** 591–602.

Bennett, M.J., Marchant, A., Green, H.G., May, S.T., Ward, S.P., Millner, P.A., Walker, A.R., Schulz, B., and Feldmann, K.A. (1996). *Arabidopsis* AUX1 gene: A permease-like regulator of root gravitropism. Science **273,** 948–950.

da Silva Conceição, A., Marty-Mazars, D., Bassham, D.C., Sanderfoot, A.A., Marty, F., and Raikhel, N.V. (1997). The syntaxin homolog AtPEP12p resides on a late post-Golgi compartment in plants. Plant Cell **9,** 571–582.

Dharmasiri, S., Swarup, R., Mockaitis, K., Dharmasiri, N., Singh, S.K., Kowalchyk, M., Marchant, A., Mills, S., Sandberg, G., Bennett, M.J., and Estelle, M. (2006). AXR4 is required for localization of the auxin influx facilitator AUX1. Science **312,** 1218–1220.

Dhonukshe, P., Baluska, F., Schlicht, M., Hlavacka, A., Samaj, J., Friml, J., and Gadella, T.W., Jr. (2006). Endocytosis of cell surface material mediates cell plate formation during plant cytokinesis. Dev. Cell **10,** 137–150.

Friml, J., Benkova, E., Blilou, I., Wiśniewska, J., Hamann, T., Ljung, K., Woody, S., Sandberg, G., Scheres, B., Jurgens, G., and Palme, K. (2002b). AtPIN4 mediates sink-driven auxin gradients and root patterning in *Arabidopsis.* Cell **108,** 661–673.

Friml, J., Vieten, A., Sauer, M., Weijers, D., Schwarz, H., Hamann, T., Offringa, R., and Jurgens, G. (2003). Efflux-dependent auxin gradients establish the apical-basal axis of *Arabidopsis.* Nature **426,** 147–153.

Friml, J., Wisniewska, J. Benková, E., Mendgen, K., and Palme, K. (2002a). Lateral relocation of auxin efflux regulator PIN3 mediates tropism in Arabidopsis. Nature **415,** 806–809.

Gälweiler, L., Guan, C., Muller, A., Wisman, E., Mendgen, K., Yephremov, A., and Palme, K. (1998). Regulation of polar auxin transport by AtPIN1 in *Arabidopsis* vascular tissue. Science **282,** 2226–2230.

Geldner, N., Anders, N., Wolters, H., Keicher, J., Kornberger, W., Muller, P., Delbarre, A., Ueda, T., Nakano, A., and Jurgens, G. (2003). The *Arabidopsis* GNOM ARF-GEF mediates endosomal recycling, auxin transport, and auxin-dependent plant growth. Cell **112,** 219–230.

Geldner, N., Friml, J., Stierhof, Y.D., Jurgens, G., and Palme, K. (2001). Auxin transport inhibitors block PIN1 cycling and vesicle trafficking. Nature **413,** 425–428.

Grebe, M., Friml, J., Swarup, R., Ljung, K., Sandberg, G., Terlou, M., Palme, K., Bennett, M.J., and Scheres, B. (2002). Cell polarity signaling in *Arabidopsis* involves a BFA-sensitive auxin influx pathway. Curr. Biol. **12,** 329–334.

Grebe, M., Xu, J., Mobius, W., Ueda, T., Nakano, A., Geuze, H.J., Rook, M.B., and Scheres, B. (2003). *Arabidopsis* sterol endocytosis involves actin-mediated trafficking via ARA6-positive early endosomes. Curr. Biol. **13,** 1378–1387.

Hugdahl, J.D., and Morejohn, L.C. (1993). Rapid and reversible high-affinity binding of the dinitroaniline herbicide oryzalin to tubulin from *Zea mays* L. Plant Physiol. **102,** 725–740.

Keller, P., and Simons, K. (1998). Cholesterol is required for surface transport of influenza virus hemagglutinin. J. Cell Biol. **140,** 1357–1367.

Lauber, M.H., Waizenegger, I., Steinmann, T., Schwarz, H., Mayer, U., Hwang, I., Lukowitz, W., and Jurgens, G. (1997). The *Arabidopsis* KNOLLE protein is a cytokinesis-specific syntaxin. J. Cell Biol. **139,** 1485–1493.

Marchant, A., Kargul, J., May, S.T., Muller, P., Delbarre, A., Perrot-Rechenmann, C., and Bennett, M.J. (1999). AUX1 regulates root gravitropism in *Arabidopsis* by facilitating auxin uptake within root apical tissues. EMBO J. **18,** 2066–2073.

Marella, M., Lehmann, S., Grassi, J., and Chabry, J. (2002). Filipin prevents pathological prion protein accumulation by reducing endocytosis and inducing cellular PrP release. J. Biol. Chem. **277,** 25457–25464.

Michaux, G., Gansmuller, A., Hindelang, C., and Labouesse, M. (2000). CHE-14, a protein with a sterol-sensing domain, is required for apical sorting in *C. elegans* ectodermal epithelial cells. Curr. Biol. **10,** 1098–1107.

Miller, R.G. (1984). The use and abuse of filipin to localize cholesterol in membranes. Cell Biol. Int. Rep. **8,** 519–535.

Morris, D.A. (2000). Transmembrane auxin carrier systems—Dynamic regulators of polar auxin transport. Plant Growth Regul. **32,** 161–172.

Morris, D.A., and Robinson, J.S. (1998). Targeting of auxin carriers to the plasma membrane: Differential effects of brefeldin A on the traffic of auxin uptake and efflux carriers. Planta **205,** 606–612.

Movafeghi, A., Happel, N., Pimpl, P., Tai, G.H., and Robinson, D.G. (1999). Arabidopsis Sec21p and Sec23p homologs. Probable coat proteins of plant COP-coated vesicles. Plant Physiol. **119,** 1437–1446.

Müller, A., Guan, C., Galweiler, L., Tanzler, P., Huijser, P., Marchant, A., Parry, G., Bennett, M., Wisman, E., and Palme, K. (1998). AtPIN2 defines a locus of *Arabidopsis* for root gravitropism control. EMBO J. **17,** 6903–6911.

Nabi, I.R., and Le, P.U. (2003). Caveolae/raft-dependent endocytosis. J. Cell Biol. **161,** 673–677.

Ottenschläger, I., Wolff, P., Wolverton, C., Bhalerao, R.P., Sandberg, G., Ishikawa, H., Evans, M., and Palme, K. (2003). Gravity-regulated differential auxin transport from columella to lateral root cap cells. Proc. Natl. Acad. Sci. USA **100,** 2987–2991.

Paciorek, T., Zazimalova, E., Ruthardt, N., Petrasek, J., Stierhof, Y.D., Kleine-Vehn, J., Morris, D.A., Emans, N., Jurgens, G., Geldner, N., and Friml, J. (2005). Auxin inhibits endocytosis and promotes its own efflux from cells. Nature **435,** 1251–1256.

Parry, G., Delbarre, A., Marchant, A., Swarup, R., Napier, R., Perrot-Rechenmann, C., and Bennett, M.J. (2001). Novel auxin transport inhibitors phenocopy the auxin influx carrier mutation *aux1.* Plant J. **25,** 399–406.

Petrasek, J., et al. (2006). PIN proteins perform a rate-limiting function in cellular auxin efflux. Science **312,** 914–918.

Pimpl, P., Movafeghi, A., Coughlan, S., Denecke, J., Hillmer, S., and Robinson, D.G. (2000). In situ localization and in vitro induction of plant COPI-coated vesicles. Plant Cell **12,** 2219–2236.

Raven, J.A. (1975). Transport of indolacetic acid in plant cells in relation to pH and electrical potential gradients, and its significance for polar IAA transport. New Phytol. **74,** 163–172.

Reinhardt, D., Pesce, E.R., Stieger, P., Mandel, T., Baltensperger, K., Bennett, M., Traas, J., Friml, J., and Kuhlemeier, C. (2003). Regulation of phyllotaxis by polar auxin transport. Nature **426,** 255–260.

Ritzenthaler, C., Nebenfuhr, A., Movafeghi, A., Stussi-Garaud, C., Behnia, L., Pimpl, P., Staehelin, L.A., and Robinson, D.G. (2002). Reevaluation of the effects of brefeldin A on plant cells using tobacco Bright Yellow 2 cells expressing Golgi-targeted green fluorescent protein and COPI antisera. Plant Cell **14,** 237–261.

Rubery, P.H., and Sheldrake, A.R. (1974). Carrier-mediated auxin transport. Planta **188,** 101–121.

Russinova, E., Borst, J.W., Kwaaitaal, M., Cano-Delgado, A., Yin, Y., Chory, J., and de Vries, S.C. (2004). Heterodimerization and endocytosis of *Arabidopsis* brassinosteroid receptors BRI1 and AtSERK3 (BAK1). Plant Cell **16,** 3216–3229.

Sabatini, S., Beis, D., Wolkenfelt, H., Murfett, J., Guilfoyle, T., Malamy, J., Benfey, P., Leyser, O., Bechtold, N., Weisbeek, P., and Scheres, B. (1999). An auxin-dependent distal organizer of pattern and polarity in the *Arabidopsis* root. Cell **99,** 463–472.

Schuck, S., and Simons, K. (2004). Polarized sorting in epithelial cells: Raft clustering and the biogenesis of the apical membrane. J. Cell Sci. **117,** 5955–5964.

Shevell, D.E., Leu, W.M., Gillmor, C.S., Xia, G., Feldmann, K.A., and Chua, N.H. (1994). EMB30 is essential for normal cell division, cell expansion, and cell adhesion in *Arabidopsis* and encodes a protein that has similarity to Sec7. Cell **77,** 1051–1062.

Spector, I., Shochet, N.R., Kashman, Y., and Groweiss, A. (1983). Latrunculins: Novel marine toxins that disrupt microfilament organization in cultured cells. Science **219,** 493–495.

Steinmann, T., Geldner, N., Grebe, M., Mangold, S., Jackson, C.L., Paris, S., Galweiler, L., Palme, K., and Jurgens, G. (1999). Coordinated polar localization of auxin efflux carrier PIN1 by GNOM ARF GEF. Science **286,** 316–318.

Swarup, R., Friml, J., Marchant, A., Ljung, K., Sandberg, G., Palme, K., and Bennett, M. (2001). Localization of the auxin permease AUX1 suggests two functionally distinct hormone transport pathways operate in the *Arabidopsis* root apex. Genes Dev. **15,** 2648–2653.

Swarup, R., et al. (2004). Structure-function analysis of the presumptive *Arabidopsis* auxin permease AUX1. Plant Cell **16,** 3069–3083.

Swarup, R., Kramer, E.M., Perry, P., Knox, K., Leyser, H.M., Haseloff, J., Beemster, G.T., Bhalerao, R., and Bennett, M.J. (2005). Root gravitropism requires lateral root cap and epidermal cells for transport and response to a mobile auxin signal. Nat. Cell Biol. **7,** 1057–1065.

Tanaka, H., Dhonukshe, P., and Friml, J. (2006). Spatio-temporal asymmetric auxin distribution: Means to coordinate plant development. Cell. Mol. Life Sci., in press.

Voigt, B., et al. (2005). Actin-based motility of endosomes is linked to the polar tip growth of root hairs. Eur. J. Cell Biol. **84,** 609–621.

Willemsen, V., Friml, J., Grebe, M., van den Toorn, A., Palme, K., and Scheres, B. (2003). Cell polarity and PIN protein positioning in *Arabidopsis* require STEROL METHYLTRANSFERASE1 function. Plant Cell **15,** 612–625.

Wiśniewska, J., Xu, J., Seifertová, D., Brewer, P., Růžička, K., Blilou, I., Roquie, D., Benková, E., Scheres, B., and Friml, J. (2006). Polar PIN localization directs auxin flow in plants. Science **312,** 883.

Xu, J., and Scheres, B. (2005). Dissection of Arabidopsis ADP-RIBOSYLATION FACTOR1 function in epidermal cell polarity. Plant Cell **17,** 525–536.

Yamamoto, M., and Yamamoto, K.T. (1998). Effects of natural and synthetic auxins on the gravitropic growth habit of roots in two auxin-resistant mutants of *Arabidopsis*, *axr1* and *axr4*: Evidence for defects in the auxin influx mechanism of *axr4.* J. Plant Res. **112,** 391–396.

Yang, Y., Hammes, U.Z., Taylor, C.G., Schachtman, D.P., and Nielsen, E. (2006). High-affinity auxin transport by the AUX1 influx carrier protein. Curr. Biol. **16,** 1123–1127.

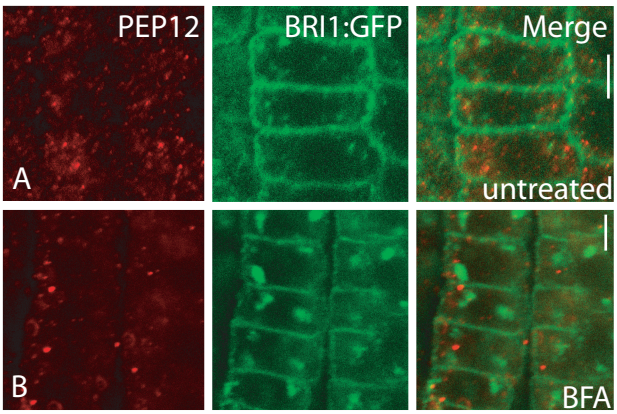

Supl. Figure 1
PVC marker PEP12 does not co-localise with endosomal marker in Arabidopsis. Non overlapping endomembranes of BRI1:GFP (green) and PEP12 (red) in untreated (A) and BFA treated (B) seedlings. Scale bars, 10µm.

A

Markers	Percentage of overlaying pixels	
PEP12/AUX1	PEP12 with AUX1 3,8 +/ - 5,2%	AUX1 with PEP12 2,1 +/ - 3,3%
ST:YFP/AUX1	ST:YFP with AUX1 45,8 +/ - 8,8%	AUX1 with ST:YFP 33,8 +/ - 4%
BRI1:GFP/AUX1	BRI1:GFP with AUX1 25,5 +/ - 3,7%	AUX1 with BRI1:GFP 30,1 +/ - 9,2%

B

Markers	Percentage of overlaying pixels	
PIN1/AUX1	PIN1 with AUX1 80,7 +/ - 4,1%	AUX1 with PIN1 34 +/ - 7,6%
ARF1/AUX1	ARF1 with AUX1 81,8 +/ - 8,9%	AUX1 with ARF1 36,6 +/ - 9,7%
BRI1/AUX1	BRI1 with AUX1 80,6 +/ - 7,9%	AUX1 with BRI1 36,9 +/ - 9,5%
γCOP /AUX1	γCOP with AUX1 81 +/ - 10,2%	AUX1 with γCOP 47,2 +/ - 11,6%

Supl. Figure 2
Merged intracellular pixel percentages are indicated for AUX1 and subcellular marker in untreated (A) and BFA treated (B) protophloem cells (n=6).

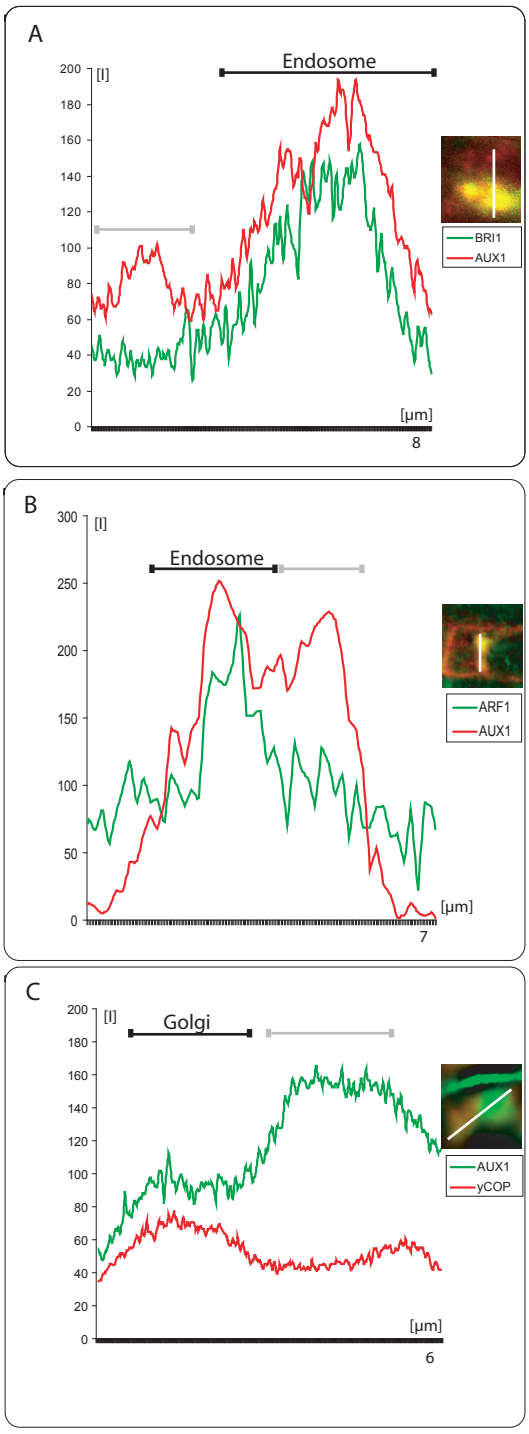

Supl. Figure 3
Intensity profile analysis AUX1 and sub-cellular markers BRI1 (A), ARF1 (B) and gamma-COP (C) in BFA compartments reveals overlapping endosomal and GA derived structures of AUX1.

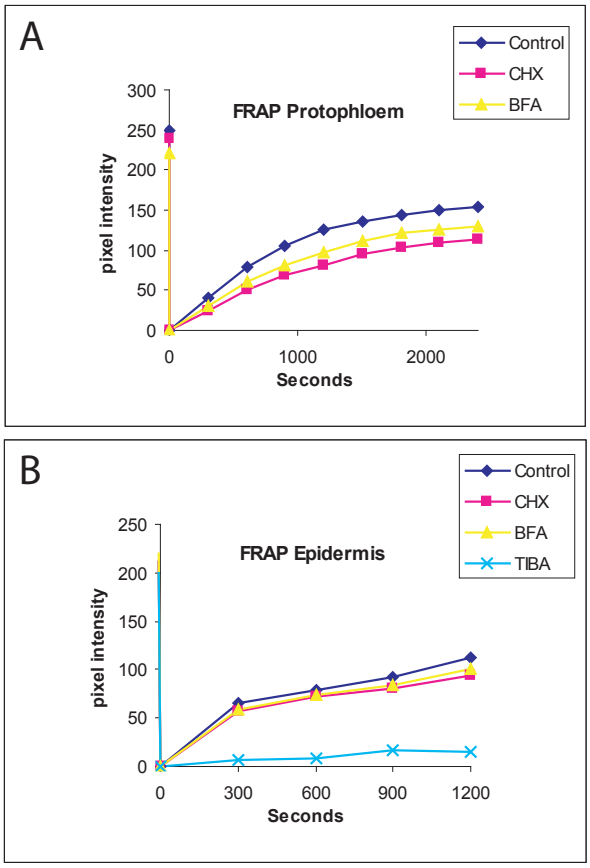

Supl. Figure 4
FRAP charts of AUX1 dynamics in protophloem (A) and epidermal cells (B) showing time dependency of AUX1 recovery at the PM.

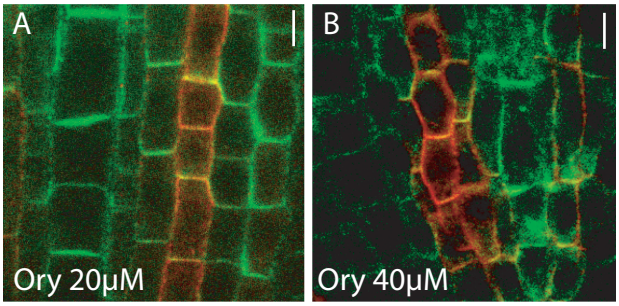

Supl. Figure 5
Oryzalin (20µM, 3 hours) treatments (A) do not interfere with AUX1/PIN1 targeting. However, higher Oryzalin concentrations (40µM, 3 hours) lead to changes in cell morphology and AUX1/PIN1 localisation

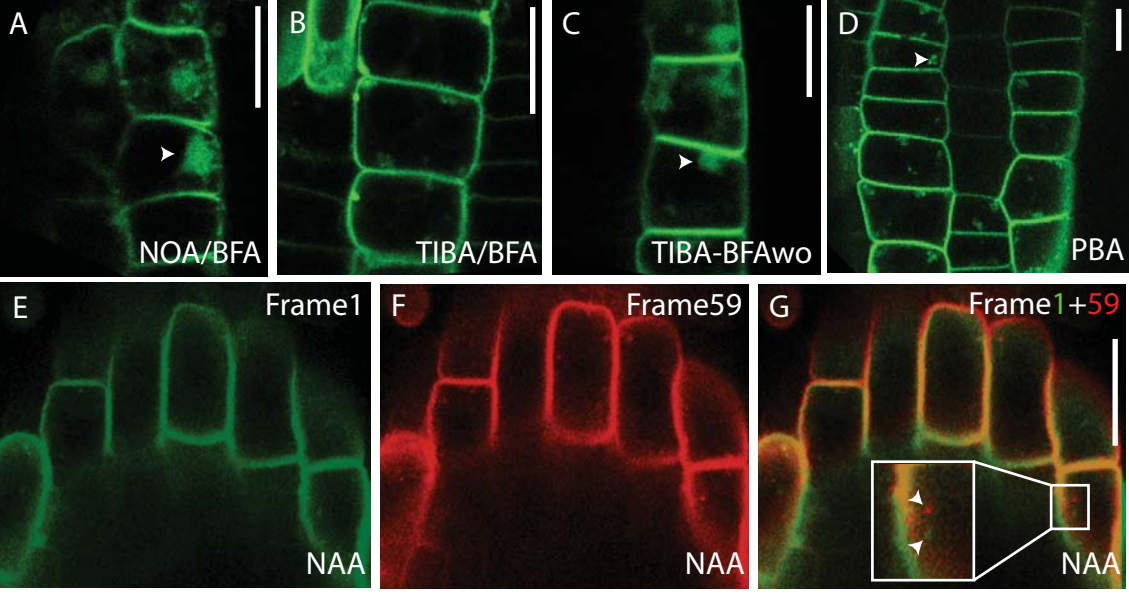

Figure S6:
(A) NOA does not interfere with AUX1:YFP accumulation in BFA compartments (see arrowhead).
(B) TIBA blocks AUX1 accumulation in BFA compartment.
(C) Removal of BFA in presence of TIBA inhibits redistribution of AUX1:YFP (see arrowhead; compare to Fig. 4A)
(D) PBA treatments show AUX1:YFP accumulations (see arrowhead).
(E-G) Auxin does not interfere with AUX1:YFP dynamics (see inset and arrowheads). Overlay of frame1 (E) and frame59 (F).
Live cell immagining of AUX1:YFP in epidermis (A-D) and lateral rootcap cells (E-F); Scale bars, 10µM.

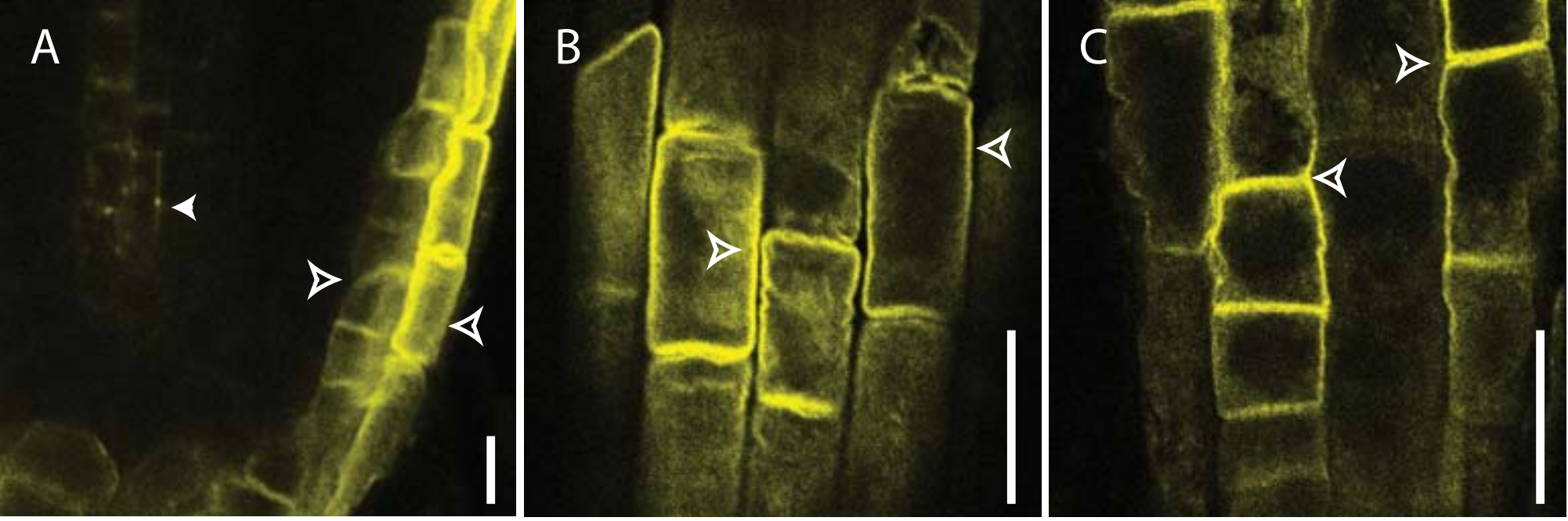

Figure S7:
(A) Filipin treated roots display AUX1:YFP miss localisation in proto-phloem- (filled arrowhead), but not in lateral root cap- (B) or epidermis cells (C) (empty arrowheads).
Live cell immagining of root cells; Scale bars, 10µM.

Legends to Movies:

Movie S1:

The movie shows dynamics of AUX1-YFP in *Arabidopsis* lateral root cap cells. Note movement of AUX1-YFP- positive structures to and from the cell surface. The movie represents 86 frames acquired at 6 sec/frame and played at 15 frames/sec.

Movie S2:

The movie shows drastically reduced dynamics of AUX1-YFP in *Arabidopsis* lateral root cap cells treated with auxin transport inhibitor TIBA 50 μM for 30 min. The movie represents 24 frames acquired at 6 sec/frame and played at 15 frames/sec.

Movie S3:

The movie shows normal dynamics of AUX1-YFP in *Arabidopsis* lateral root cap cells treated with excess auxin (NAA 10 μM) for 30 min. The movie represents 59 frames acquired at 6 sec/frame and played at 15 frames/sec.